ICSV14
Cairns • Australia
9-12 July, 2007

BEARING PROFILE AND MISALIGNMENT EFFECTS ON THE VIBRATION BEHAVIOUR OF ROTATING MACHINERY

Ningsheng Feng and Eric Hahn

School of Mechanical and Manufacturing Engineering, University of New South Wales
Sydney, NSW 2052, Australia
n.feng@unsw.edu.au

Abstract

The vibration behaviour (eg. unbalance response, stability) of rotating machinery consisting of flexible rotors supported by hydrodynamic or fluid film bearings is significantly affected by the dynamic characteristics of the bearings. These characteristics depend on bearing parameters such as length, diameter, nominal clearance, rotor speed and oil viscosity, as well as the bearing reaction load (which depends on the relative transverse alignment of the bearings in statically indeterminate systems). Hence, various bearing profiles are used in practice and care is taken in setting the relative bearing positions during installation in order to improve dynamic performance, prolong service life and enhance productivity.

There are two types of bearing clearance profiles used in practice: the multi-lobe type consisting of two or more lobes (pads) with defined pad curvature centres which need not coincide with the bearing centre; or the wave type with variable curvatures normally defined by some functions. Investigated here theoretically is the effect of the first type of profile (including axial groove, elliptic, 3 lobe, and 2 or 3 pad offset bearings) and the effect of lateral misalignment on the vibration behaviour of the machinery.

For any particular profile, the dynamic characteristics of the bearings are obtained via a numerical solution of the Reynolds equation, a partial differential equation describing the pressure distribution in the fluid film. Sample results show how different bearing clearance profiles and different degrees of lateral misalignment affect the natural frequencies, stability thresholds and unbalance response of simple statically indeterminate rotor bearing systems (systems with more than two bearings). Among the bearings investigated, under the assumed conditions of the numerical examples, different bearing profiles are shown to have different effects on the stable system performance due to bearing misalignment.

1. INTRODUCTION

Turbomachinery is generally supported by fluid film bearings. The hydrodynamics of these bearings play an important role in the performance of the machinery [1]. The bearings have no contact between the solid surfaces at normal running conditions, as shown in Fig. 1. Instead, lubricant pressures developed in the clearance between the journal and bore provide

the load capacity for the bearing. The governing equation for determining the pressures developed in such bearings is the Reynolds equation [2]:

$$\frac{\partial}{\partial X}\left(h^3\frac{\partial p}{\partial X}\right)+\frac{\partial}{\partial Z}\left(h^3\frac{\partial p}{\partial Z}\right)=-6\mu U\frac{\partial h}{\partial X}+12\mu V=12\mu\left(\frac{\omega}{2}\frac{\partial h}{\partial \psi}+\frac{\partial h}{\partial t}\right)=-12\mu\left[\left(\dot{z}-\frac{\omega}{2}y\right)\sin\psi+\left[\dot{y}+\frac{\omega}{2}z\right]\cos\psi\right] \quad (1)$$

Integration of the pressures gives the fluid film forces:

$$\begin{pmatrix}F_y\\F_z\end{pmatrix}=-\int_{\psi_1}^{\psi_2}\int_{-L/2}^{L/2}p\begin{pmatrix}\cos\psi\\\sin\psi\end{pmatrix}RdZd\psi=\begin{pmatrix}0\\W\end{pmatrix} \quad (2)$$

The nondimensional forms of eqs (1) and (2) are

$$\frac{\partial}{\partial\psi}\left(\bar{h}^3\frac{\partial\bar{p}}{\partial\psi}\right)+\left(\frac{D}{L}\right)^2\frac{\partial}{\partial\bar{Z}}\left(\bar{h}^3\frac{\partial\bar{p}}{\partial\bar{Z}}\right)=-2\left[\left(\bar{z}'-\frac{\bar{y}}{2}\right)\sin\psi+\left(\bar{y}'+\frac{\bar{z}}{2}\right)\cos\psi\right] \quad (3)$$

and

$$\begin{pmatrix}\bar{F}_y\\\bar{F}_z\end{pmatrix}=-3\int_{\psi_1}^{\psi_2}\int_{-L/2}^{L/2}\bar{p}\begin{pmatrix}\cos\psi\\\sin\psi\end{pmatrix}d\bar{Z}d\psi=\begin{pmatrix}0\\1/\pi S\end{pmatrix} \quad (4)$$

respectively.

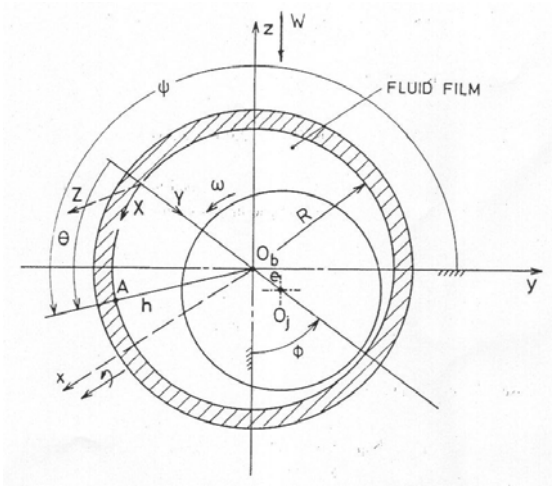

Figure 1: Bearing schematic

It can be seen from eq. (1) or (3) that the solution of the Reynolds equation is very sensitive to the film thickness *h* which in turn is specified by the clearance profiles of the bearing. Different bearings in practice use different clearance profiles to achieve different dynamic performance. The shaft journals are circular. Different clearance profiles are achieved by varying the bearing bore shapes. There are two common types of bearing pads used in fluid film bearings [3]: tilting pads or fixed pads. The former has the pads pivoting automatically according to the pressure distribution; while the latter consists of various bearing bore shapes ranging from the plain circular to sophisticated wave functions. Within the fixed pad bearing classification, the geometry of the pads is generally further categorised into those with variable curvatures defined by some mathematic function, or pads with constant radii of curvature but variable pad extents and offset centres of curvature. This paper focuses on the characteristics of the bearings in the latter subgroup ie. bearings containing fixed pads with given pad curvatures. These bearings include plain journal bearings with axial grooves, elliptical (2 pads or lobes) or multi-lobe bearings, offset bearings, and pocket bearings [4].

2. APPROACH

In analysing a multi-pad bearing, Reynolds equation is solved for each individual pad with appropriate pressure boundary and cavitation conditions to give the resultant film forces acting at that pad. The resultant force from all the pads corresponds to the bearing load in both magnitude and direction. A general approach is adopted which caters for all multi-lobe bearings (including elliptical and axial groove bearings), all offset bearings, or even combinations of the two. The pads may have different pad extents and centre of curvature positions but the radii of the pads are generally the same, though do not have to be.

Starting with the simple case of the elliptical bearing, as shown in Fig. 2, the bottom and top pads have their centres of curvature at O_b and O_t respectively [3]. From the geometry

$$\varepsilon_{b,t}^2 = \varepsilon^2 + \delta_{b,t}^2 \pm 2\delta_{b,t}\varepsilon\cos\phi' \tag{5}$$

$$\phi'_{b,t} = \tan^{-1}\frac{\varepsilon\sin\phi'}{\varepsilon\cos\phi' \pm \delta_{b,t}} \tag{6}$$

where $\pm$ refers to bottom or top pad respectively. The pad starting angles from horizontal *y'*

$$\psi'_{1b,t} = \gamma_{b,t} - \psi_{12b,t}/2 + \pi/2 \tag{7}$$

where $\gamma_{b,t}$ = 180° and 0° respectively.

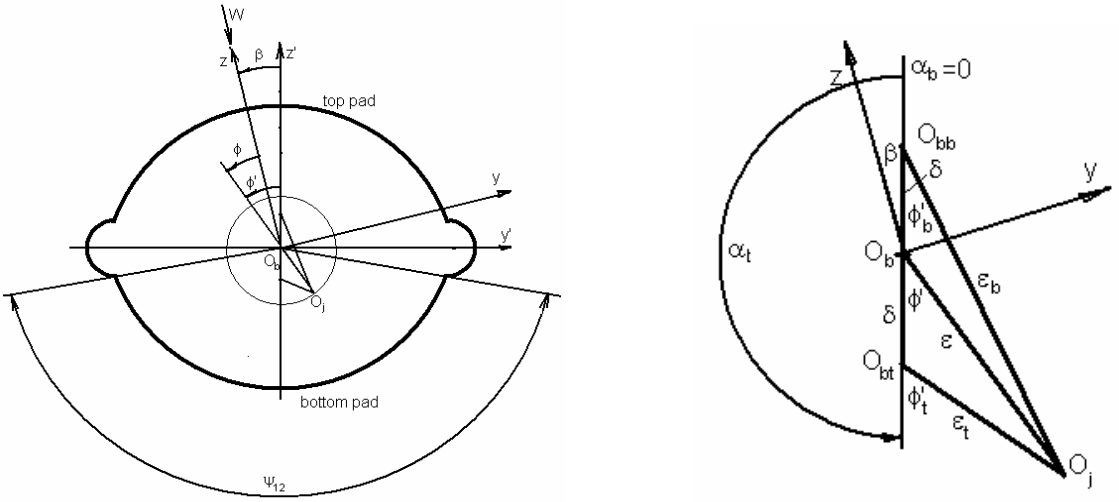

Figure 2: Geometric relationship for elliptic bearings

The required parameters are the aspect ratio *L/D*, the eccentricity ε, the load inclination angle β, as well as the number of pads n = 2, followed by 2 sets of pad information: pad extent $\psi_{12b,t}$ (<180°), mid-pad positions $\gamma_{b,t}$ (180° and 0° from vertical up), ellipticities $\delta_{b,t}$, and pad centres of curvature directions $\alpha_{b,t}$ (0° and 180° from vertical up).

Similarly, for a 2-pad offset bearing as indicated in Fig. 3

$$\varepsilon_{b,t}^2 = \varepsilon^2 + \delta_{b,t}^2 - 2\delta_{b,t}\varepsilon\cos\left(90^\circ \pm \phi'\right) \tag{8}$$

$$\phi'_{b,t} = \tan^{-1}\frac{\varepsilon\sin\phi' \pm \delta_{b,t}}{\varepsilon\cos\phi'} \tag{9}$$

and the expression for $\psi'_{1b,t}$ is the same as eq. (7).

Note that if the direction of rotation is reversed (or the pads are offset in the opposite directions), the signs $\pm$ in eqs (8) and (9) will be changed to $\mp$.

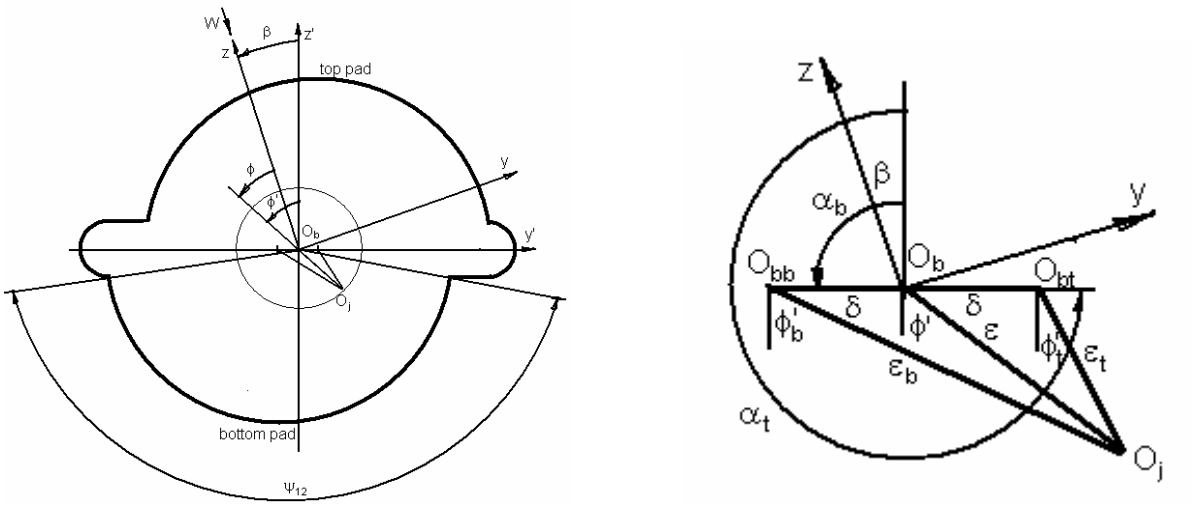

Figure 3: Geometric relationship for 2-pad offset bearings

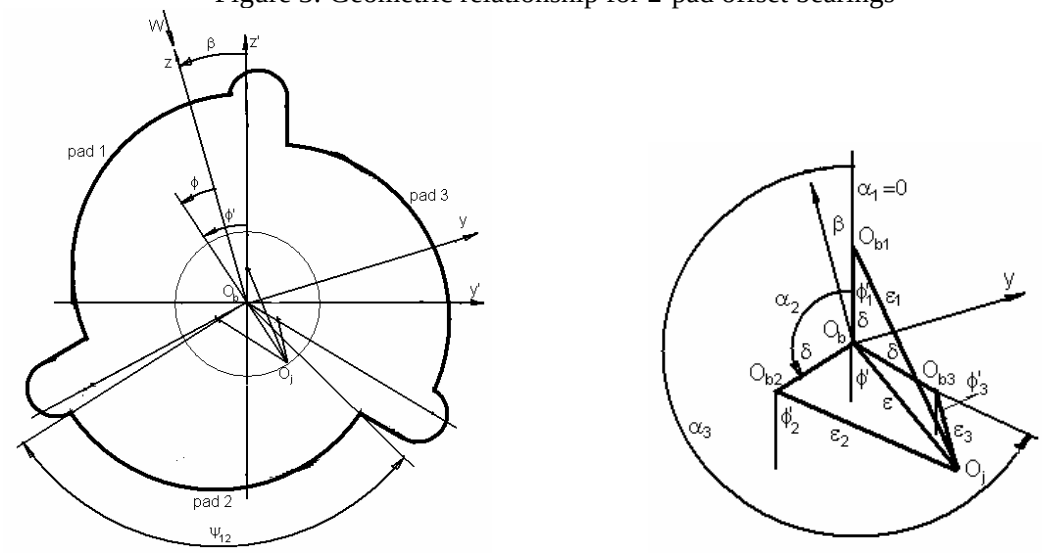

Figure 4: Geometric relationship for 3-pad offset bearings

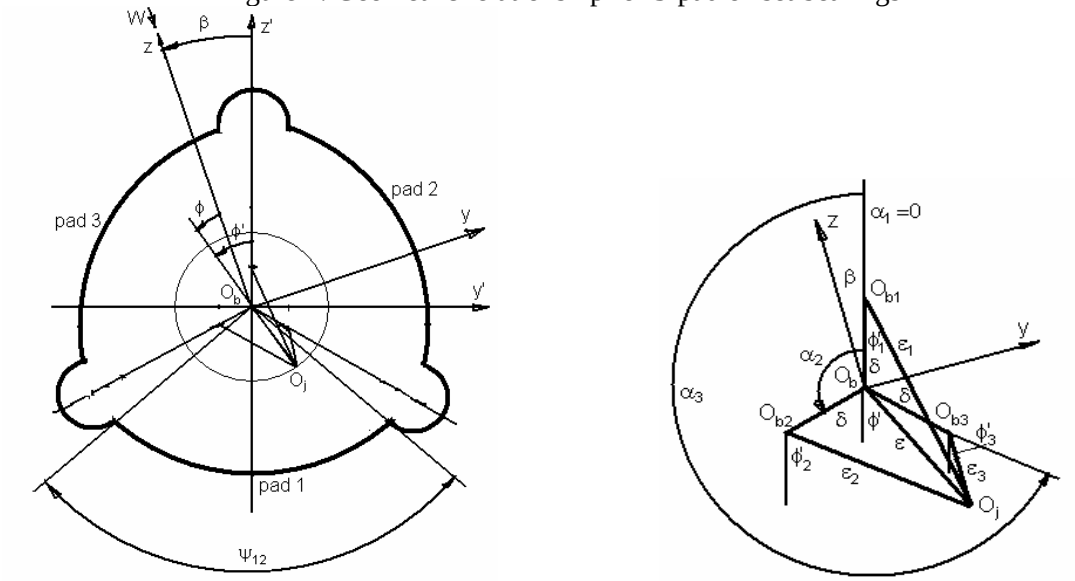

Figure 5: Geometric relationship for 3-lobe bearings

For 3-pad offset bearings and 3-lobe bearings with identical pads, the geometric relationships are shown in Figs 4 and 5 respectively, and the pad eccentricity, attitude angle and pad starting angle expressions are

$$\varepsilon_i^2 = \varepsilon^2 + \delta_i^2 + 2\delta_i \varepsilon \cos(\alpha_i - \phi') \tag{10}$$

$$\phi'_i = \tan^{-1} \frac{\varepsilon \sin \phi' + \delta_i \sin \alpha_i}{\varepsilon \cos \phi' + \delta_i \cos \alpha_i} \tag{11}$$

$$\psi'_{1i} = \gamma_i - \psi_{12i}/2 + \pi/2 \tag{12}$$

respectively.

Equations (10-12) are general and can also be applied to the elliptical (including axial groove) and 2-pad offset bearings as long as appropriate pad centre angles α_i are applied. Table 1 lists the ranges of bearing specific parameters, for bearings with up to three pads for the bearings analysed here, assuming identical pads and symmetrical pad arrangement. Note that these assumptions are not constraints to the general software capabilities.

Table 1: Sample bearing parameters (deg.)

Bearing Type	Pad Extent ψ_{12}	Position γ	Centre α
Elliptic/axial groove	<180	180, 0	0, 180
2-pad offset [1]	<180	180, 0	90, -90
3-pad offset [1]	<120	60, 180, -60	0, 120, 240
3-lobe	<120	180, -60, 60	0, 120, 240

[1] Signs of α reverse if rotor rotation is clockwise (Figs 3 and 4)

3. SOLUTION PROCEDURE

For given eccentricity ratio ε, load inclination β, and guessed attitude angle ϕ, the finite difference method is used to solve the Reynolds equation for each pad. The simultaneous equations for the pressures are solved iteratively using successive over-relaxation. During the iterations, if a pressure value falls below the cavitation pressure p_{cav}, it is truncated to p_{cav} immediately, resulting in the Reynolds cavitation boundary condition (zero pressure gradient at p_{cav}). The converged pressure values are then integrated to obtain the fluid film force components for that pad. The sum of the force components from all pads in the direction perpendicular to load W should be zero. The interval halving method is adopted to iteratively find the correct attitude angle ϕ.

4. RESULTS AND DISCUSSION

Figure 6 is a schematic of a simple rotor bearing system (similar to that in [6] but supported by different bearings) used in the numerical studies. Note the different coordinate systems in Figs 1 and 6. The superimposed unbalance distribution (10 g.cm each in vertical and horizontal directions at the two disks respectively) is the unbalance input for the frequency response calculations. Each of the rotors is symmetric and the bearings are identical. Table 2 summarises the relevant rotor data and the bearing data for plain journal bearings. Some bearing static parameters and dynamic bearing coefficients for various bearings as functions of the eccentricity ε and/or load inclination angle β are presented in [5]. These bearing parameters are tabulated and inputted into the vibration analysis software to study the effects of the bearing profiles and misalignment on the vibration behaviours of the rotor systems supported by more than two bearings. Also included for comparison purposes are the results for plain journal bearings.

Figure 7 shows the Campbell diagrams as well as the stability thresholds for the aligned rotor systems supported by the plain circular journal bearings. In the frequency range of interest, there are seven relevant natural frequencies. Of these, five are forward modes (first, third, fourth, fifth and sixth) and two are backward modes (second and seventh). The synchronous frequency line intersects with two of the forward modes (the first and sixth), resulting in two critical speeds. In the frequency range of interest, all the modes are stable with negative real parts in the complex natural frequencies, except for the first mode (1+) which has positive real part above the corresponding stability thresholds. Campbell diagrams for systems supported by other bearings are similar with different natural frequency values. The stability thresholds are listed in Table 3. It is seen that different bearing profiles exhibit different natural frequencies and stability thresholds, thereby altering the system dynamic behaviour. In particular, similar to the findings in [7], the 3-pad offset bearings provide a remarkably stable system (having approximately double the stability thresholds of the others), followed by the elliptical and 2-pad offset bearings. As expected, the plain journal bearings are least stable.

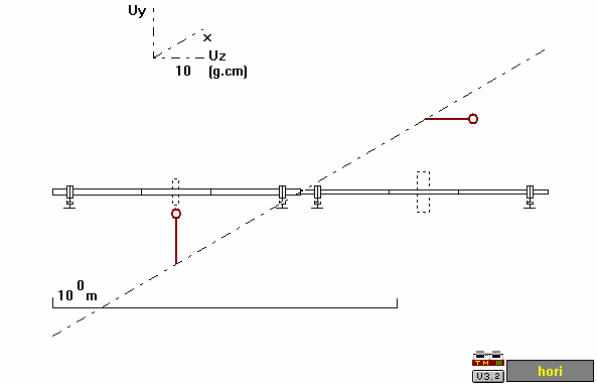

Figure 6: Sample rotor bearing system (18 segments)

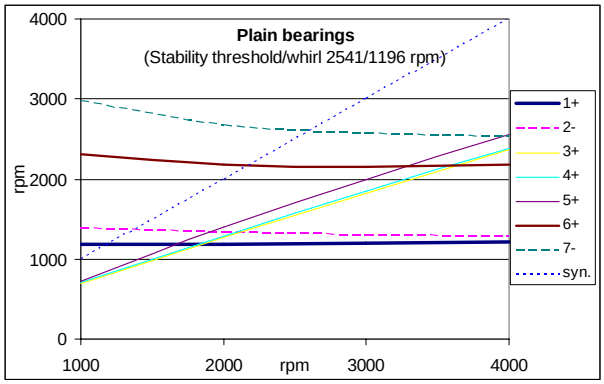

Figure 7: Campbell diagram and stability threshold (Plain bearings)

Table 2: Sample rotor and bearing data

Rotor: E = 210 GPa, G = 80 GPa, density = 7850 kg/m^3, $m_{disk\ 1}$ = 5.2kg, $m_{disk\ 2}$ = 9.2kg Bearings: Length = 0.018 m, Diameter = 0.036 m, Clearance = 90 μm, Viscosity = 0.014 Pa.s		
Segment	Length (m)	Diameter (m)
1, 9	0.041	0.020
2-3, 7-8, 11-12, 16-17	0.009	0.036
4-6	0.200	0.020
10, 18	0.041	0.015
13-15	0.200	0.015

Table 3: Stability thresholds and whirl frequencies (rpm)

Bearing	Threshold	Whirl freq.
Plain	2541	1196
Axial	2529	1185
Elliptic	3258	1248
3-lobe	2858	1277
2-pad offset	3228	1240
3-pad offset	6572	1232

Figure 8 shows the linearised unbalance responses at the disks for the unbalance distribution shown in Fig. 6 for the rotors supported by the plain circular journal bearings. The responses confirm the two critical speed peaks encountered. Responses for systems supported by other bearings show similar trends with different resonance peak amplitudes at slightly different critical speeds. Table 4 shows the misalignment effects on the stability (system damping) of the systems supported by different bearings. The real parts of the 1+ mode under the aligned bearing configuration at the rotor speed of 3000rpm (shown in the centre in bold) are used as reference. The third bearing from left in Fig. 8 is then misaligned by $\delta = 0.5$ (half of the nominal bearing radial clearance) in horizontal and/or vertical directions, and the corresponding values of the real parts of the 1+ modes are recorded for comparison. If the values are more negative than those for the reference case, the system is more stable;

otherwise, it is more unstable. From the table, it can be seen that for the chosen rotors and running conditions, the effects are different. For plain circular bearings, misalignment in +*y* or +*z* directions only improves the stability, while the axial groove circular bearings, elliptical bearings and 3-pad offset bearings favour misalignment in +*z* direction in general but 3-lobe bearings prefer misalignment in +*y* direction. It is interesting to note that for 2-pad offset bearings, any misalignment direction except for –*y* will improve the stability. However, different running conditions or misalignment at different bearings may change the outcomes.

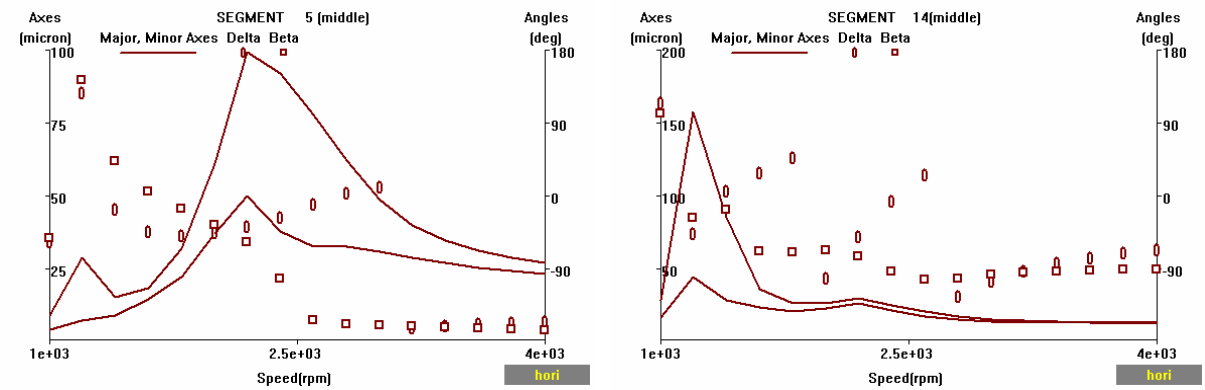

Figure 8: Frequency responses (major and minor axes of elliptic orbits) at the two disks (Beta: response phase angles; Delta: orientation angles of major axes from *y* [8])

Table 4: Effect of bearing misalignment on the real part of the 1+ mode (ω=3000rpm)

(0.5,-0.5) (0.,-0.5) (-0.5,-0.5)	(+0.5,0.) **Aligned** (-0.5,0.)	(+0.5,+0.5) (0.,+0.5) (-0.5,+0.5)	<- misalignment (B_{y3}, B_{z3})
1.146 *1.576* *2.793*	0.8940 **1.017** *1.945*	*1.109* 0.8443 *1.249*	<- Plain bearings
0.9531 *1.521* *2.576*	0.7152 **0.9191** *1.771*	0.7235 0.7338 0.6955	<- Axial groove
-0.7928 0.2090 1.687	-0.7972 **-0.5647** 0.4066	*-0.5070* *-0.00059* *-0.1285*	<- Elliptic
-0.5752 -0.2396 *1.201*	0.1557 **0.4057** *1.153*	0.4033 *0.4111* *0.4772*	<- 3-lobe
-0.9033 *-0.5500* *0.2433*	*-1.287* **-1.629** -1.883	-2.039 -2.418 -3.390	<- 3-pad offset
-0.4851 -0.4497 -0.9438	-0.3738 **-0.2538** *-0.0508*	-0.7072 -0.5354 -0.8256	<- 2-pad offset

6. CONCLUSIONS

A general approach has been developed to analyse the bearing characteristics with fixed pads separated by axial grooves. Different clearance profiles result in different static and dynamic coefficients, and hence affect the dynamic behaviour of the supported rotor bearing systems. Also, the bearings involved generally show load orientation dependent characteristics and corresponding bearing coefficients are needed if the bearing loads are non-vertical, as could

occur in statically indeterminate rotor systems, or in rotor systems subjected to other than just gravitational radial loads.

Numerical results show how different clearance profiles and different degrees of lateral misalignment affect the natural frequencies, stability thresholds and unbalance response of simple statically indeterminate rotor bearing systems. Among the bearings investigated, under the assumed conditions of the numerical examples, different bearings have different effects on the stable system performance due to bearing misalignment. No general trend for the misalignment effect is detected and individual investigations should be performed for each rotor bearing system.

7. NOMENCLATURE

C radial clearance
D bearing diameter $= 2R$
d offset
e eccentricity
F fluid film force $\bar{F} = F / \pi WS$
h film thickness, $= C - z\sin\psi - y\cos\psi, \quad \bar{h} = h / C$
L bearing length
n number of pads
p pressure $\bar{p} = p(C/R)^2 / 6\mu\omega$
R bearing radius
S Sommerfeld number $= (R/C)^2 \mu\omega RL / \pi W$
t time
U, V velocity components at the journal surfaces
W load
X, Y, Z Cartesian coordinates at bearing surface
x, y, z Cartesian coordinates at bearing centre
α pad curvature centre direction from vertical up
β load inclination angle from vertical up
δ nondimensional offset $= d / C$
ε nondimensional eccentricity $= e / C$
ϕ attitude angle from load
ϕ' attitude angle from vertical up $= \phi + \beta$
γ pad angular position (mid-point) from vertical up
μ viscosity
ψ angular coordinate
ψ_{12} pad extent
ω rotor speed

Superscripts (if not otherwise defined)
¯ nondimensional
· differentiation with respect to real time *t*
' differentiation with respect to nondimensional time ωt

Subscripts (if not otherwise defined)
b, t bottom, top pad
i i'th pad
1, 2 starting, finishing

REFERENCES

[1] J.W. Lund, "Stability and damped critical speeds of a flexible rotor in fluid-film bearings", *Trans. ASME, Journal of Engineering for Industry*, Series B, V. **96**, No. **2**, 509-517, (1974).
[2] O. Pinkus, and B. Sternlicht, THEORY OF HYDRODYNAMIC LUBRICATION, *McGRAW HILL*, (1961).
[3] N.S. Feng and E.J. Hahn, "Computation of bearing characteristics: elliptic bearings and tilting pad bearings", Report 1993/AM/3, UNSW, (1993).
[4] N.S. Feng and E.J. Hahn, "Analysis of Hydrodynamic Fluid Film Pocket Journal Bearings", *STLE 60th Annual Meeting and Exhibition*, Las Vegas, (2005).
[5] N.S. Feng and E.J. Hahn, "Effect of Clearance Profile of Hydrodynamic Fluid Film Bearing on the Vibrations of Rotating Machinery", 2nd International Conference, Lanzhou, 6pp, (2007).
[6] Y. Hori and R. Uematsu, "Influence of misalignment of support journal bearings on stability of a multi-rotor system", *Tribology International*, 249-252, (1980).
[7] D.R. Garner, C.S. Lee and F.A. Martin, "Stability of profile bore bearing: influence of bearing type selection", *Tribology International*, 204-210, (1980).
[8] N.S. Feng and E.J. Hahn, "Programs for rotor dynamic analysis using transfer matrix method", Report 1988/AM/2, UNSW, (1988).